

Investigation of the Anti-tubercular Potential of Selected Phytochemicals Using Computational Approach

Vikas Jha^{1,*}, Ajit Kumar¹, Geetika Preman², Kunal Gharat², Muskaan Mulani², Shalmali Pendse¹, Kabir Thakur¹, Anjali Bhosale¹, Siddhartha Pandya², Arpita Marick¹

¹National Facility for Biopharmaceuticals, Guru Nanak Khalsa College, Mumbai, India

²Department of Five-Year Integrated Course in Bioanalytical Sciences, Guru Nanak Khalsa College, Mumbai, India

Email address:

vikasjjha7@gmail.com (V. Jha)

*Corresponding author

To cite this article:

Vikas Jha, Ajit Kumar, Geetika Preman, Kunal Gharat, Muskaan Mulani, Shalmali Pendse, Kabir Thakur, Anjali Bhosale, Siddhartha Pandya, Arpita Marick. Investigation of the Anti-tubercular Potential of Selected Phytochemicals Using Computational Approach. *Biomedical Statistics and Informatics*. Vol. 7, No. 2, 2022, pp. 31-40. doi: 10.11648/j.bsi.20220702.13

Received: May 31, 2022; Accepted: June 20, 2022; Published: June 30, 2022

Abstract: While tuberculosis is a curable disease, *Mycobacterium tuberculosis* (*M. tb*), its etiological agent, remains a major human pathogen. For thousands of years of human life, this pathogen leads to more human deaths than any other infectious agent. Relatively affordable new drugs for the treatment of this lethal disease need to be developed in light of global TB infections. The current study aims to screen a broad spectrum of bioactive compounds, along with standard anti-tubercular drugs against Topoisomerase II protein of *Mtb*. The Lipinski rule was employed for the initial screening of the phytochemicals based on their pharmacokinetic properties. The 75 shortlisted compounds were subjected to molecular docking analysis with the Topoisomerase II receptor, which revealed six molecules Glyceollin-I, Fumarine, Chelidonine, Alstonine, Tuberosin, and Asarinin, as potential inhibitors against the receptor. Furthermore, the toxicity profiles of these six compounds were evaluated, and Glyceollin-I, Alstonine, and Tuberosin were shown to be the safest as compared to the others. The MD simulation analyses of these compounds in complexation with the receptor confirmed that the receptor-Alstonine complex was the most stable. Thus, the findings of our study will contribute to a better understanding of the Mycobacterial Topoisomerase II protein target and pave the way for the development of a novel therapeutic candidate drug to treat this disease.

Keywords: Bioactive Compounds, Molecular Docking, MD Simulations, *Mycobacterium tuberculosis*, Topoisomerase II Receptor

1. Introduction

Tuberculosis (TB) is a major communicable disease caused by infection by *Mycobacterium tuberculosis* (*M. tb*) bacteria. One-third of the global population is estimated to be infected with *M. tb* making it one of the top 10 causes of death worldwide. The inability of the BCG vaccine to provide complete protection against pulmonary TB in adults and the emergence of drug-resistant tuberculosis is the main reason for such a massive death toll. Therefore, there is a huge need for the development of newer or alternate therapies to circumvent the global risk [1].

Due to the emergence of drug-resistant strains of *M. tb*, the research on newer drug discovery remains at the forefront.

Various approaches are being used for the discovery of anti-tubercular candidates. Approaches like repurposing, target-based screening, optimization of chemical scaffolds of the known drugs, targeting the pathogen virulence factors, signal mechanisms, and targets related to the establishment of mycobacterial dormancy in the host's macrophages seem to be promising. Currently available anti-TB drugs are mostly targeted at metabolic pathways and proteins, which are essential for the growth of *M. tb* [2-4].

The genome of *M. tb* comprises approximately 3950 genes and of which only about 10% (461 genes) are required for the growth and survival of the bacilli *in vitro* under aerobic growth conditions. Amongst these essential genes, 15 genes encode components of the DNA replication machinery, out

of which effective inhibitory agents are available only for a small number of essential proteins. DNA gyrase is the only clinically validated target of the fluoroquinolones used in the treatment of MDR-TB [5]. Previous studies have shown the success of fluoroquinolones and the existence of other exploitable ligand-binding pockets in gyrase suggesting the importance of new gyrase-specific inhibitors. In a study by Rahimi et al. 2016 [6], the antibiotic compound Simocyclinone D8 (SD8) was found to inhibit both gyrase DNA binding and supercoiling reaction, hence it acts as a competitive inhibitor for DNA binding sites. Using this mechanism of inhibition, structural similarity search and molecular docking studies were carried out to identify new molecules for DNA gyrase inhibition using SD8 structure. Another investigation in the past conducted by Setzer et al [7], involved screening of 561 known antibacterial phytochemicals listed in the *Dictionary of Natural Products* with the help of docking studies with six bacterial protein targets (peptide deformylase, DNA gyrase/topoisomerase IV, UDP-galactose mutase, protein tyrosine phosphatase, cytochrome P450 CYP121, and NAD⁺-dependent DNA ligase) of *E. coli*, out of which peptide deformylase (EcPDF), *E. coli* topoisomerase IV (EcTopoIV), and *E. coli* DNA ligase (EcLigA) were found to be most susceptible protein targets, based upon docking energies, for phytochemical ligands. Khan et al [8] also worked on the structural modifications in templates obtained from natural sources that contribute to better activity like cyclothialidines and haloemodin analogs to treat bacterial infections. Previously, studies have revealed that we can discover a novel scaffold of DNA gyrase inhibitors by combining multiple machine learning methods and target-based approaches [9].

The type II topoisomerase, DNA gyrase, functions in relieving torsional strain, during the process of chromosomal DNA replication by carrying out controlled alterations of the DNA topology to ensure processive synthesis. The presence and essentiality of gyrase in all bacteria and its absence from most eukaryotes (exceptions include plants and plasmodia) make it an ideal target for antibacterial agents. In the history of antibiotics, DNA gyrase has been proven as one of the most successful drug targets [5].

DNA topoisomerases are broadly classified as type I (which make transient single-stranded breaks in DNA) and type II (transient double-stranded breaks) depending on their mechanism of action. Every species has at least one enzyme from each type of DNA topoisomerases due to their functional importance. In organisms with additional topoisomerases, all the topoisomerases are not essential for the cell survival, but *M. tb* genome encodes for only a single type I (topo I; gene = Rv3646c) and a single type II topoisomerase [gyrase; genes = Rv0006 (gyrA) and Rv0005 (gyrB)], which is responsible for the decatenation, relaxation, and supercoiling. Due to this, *M. tb* gyrase has been extensively exploited as a potential antibacterial target. The availability of extensive structural information on gyrase from several bacteria, including *M. tb*, enables in-silico methods to screen for gyrase-specific inhibitors [10].

Newer antimycobacterial drugs are required to efficiently treat drug-resistant forms of *M. tb* and eradicate the latent infection. Even today, traditional remedies continue to play an important role in modern medicine wherein approximately 80% of the world's inhabitants rely on them as their primary health-care. The amalgamation of traditional medicine and modern science may provide newer and valuable, affordable, safe, novel, and effective therapies [11]. Therefore, the present study focuses on virtual screening approach to discover novel drug candidates against Topoisomerase II receptor. A list of bioactive compounds was screened based on their pharmacokinetic and pharmacological properties. Further, these druggable compounds were then docked with the receptor to identify the potential drug candidates. Moreover, for a comparative evaluation, certain standard anti-tubercular drugs were studied as controls.

2. Materials and Method

2.1. Data Retrieval

The virtual screening was performed on the three-dimensional structure of a topoisomerase II complex (5BTC) of *Mtb*, retrieved from the RCSB PDB data repository [12], a worldwide library for high-definition 3D structural data. A list of 302 natural antitubercular compounds from various classes of phytochemicals was retrieved from Dr. Duke's library [13], which is a comprehensive database for phytochemicals. The three-dimensional structure of respective ligands was retrieved from the PubChem database (<https://pubchem.ncbi.nlm.nih.gov/>). Further, the structures were converted to PDB format using PyMol, an open-source molecular visualization tool [14].

2.2. Pharmacokinetics, Bioavailability and Drug-Likeliness Prediction

Theoretical prediction of pharmacokinetic properties of drug-like compounds from their molecular structures was carried out using SwissADME web-based tool (<http://www.swissadme.ch/>). Since high binding efficiency and low toxicity profile of a compound cannot be the only criterion to consider a lead molecule as a potential drug candidate, therefore, it is essential to have a pharmacokinetic profile that can aid in the discovery of new lead molecules. For preliminary screening, Lipinski's rule of five parameters was employed. For a compound to qualify as a ligand, it should have a molecular mass of less than 500 Daltons, an octanol-water partition coefficient (log P) that does not exceed 5, less than 10 H-bond donors, no more than 5 hydrogen bond donors (the total number of nitrogen-hydrogen and oxygen-hydrogen bonds). Any molecule violating the Lipinski rule of five was exempted from further analysis (Lipinski, 2004). Apart from pharmacokinetic properties, the SwissADME tool forecasts bioavailability radar based on several physicochemical properties. These properties assist in the detection of drug-likeness and the molecule's suitability for oral use. The properties which assist in bioavailability radar are

Lipophilicity, Molecular size, Polarity, Insolubility, Instauration, and Flexibility. The range of each parameters is mentioned as LIPO, Lipophilicity: $-0.7 < \text{XLOGP3} < +5$; SIZE, Molecular size: $150 \text{ g/mol} < \text{mol. wt.} < 500 \text{ g/mol}$; POLAR, Polarity: $20 \text{ \AA}^2 < \text{TPSA} < 130 \text{ \AA}^2$; INSOLU, Insolubility: $0 < \text{Log S (ESOL)} < 6$; INSATU, Instauration: $0.25 < \text{Fraction Csp3} < 1$; FLEX, Flexibility: $0 < \text{Number of rotatable bonds} < 9$. Any deviation from the mentioned parameters indicates that the ligand is unfit for oral consumption [15].

2.3. Molecular Docking

The virtual screening process was initiated with the step of pre-processing of the receptor, which includes removal of ligands, heteroatoms, nucleic acid groups, and water molecules using Discovery Studio 2020. To the pre-processed structure of the receptor (Figure 1), Kollman charges were added, followed by the addition of polar hydrogen atoms, and the final output was saved in PDBQT format. While the preparation of the ligand consists of a series of energy minimization steps that generate structure variation and optimization and the output was saved as PDBQT format using AutoDock Tools [16].



Figure 1. Pre-processed three-dimensional structure of the Topoisomerase II complex of the *Mycobacterium tuberculosis*.

The selected ligand structures were docked with the receptor in AutoDock Vina [17]. The AutoDock Vina software performs the prediction of bound confirmation based on free binding energies, which was calculated based on the empirical force field. The grid box was set at 19.719, 11.930, and 25.015 Å to dock the selected ligands against the target, and the box size was set at 40, 40, and 40 Å in x, y, and z directions, respectively. Discovery Studio Visualizer 2020 was used to evaluate the interactions between the receptor-ligand complexes.

2.4. Toxicity Prediction

Toxicity is an important indication of the drug candidate's behaviour, fate, and level of toxicity in the human body. ProTox II [18] tool was employed to calculate the likely

toxicity profiles, toxicity class, and LD50 values of the shortlisted phytochemicals. Based on the LD50 value of 3700 dataset compounds, it determines the toxicity of the compound and categorizes the query drug into six broad groups, with Class I being extremely toxic and Class VI being safest.

2.5. Molecular Dynamic Simulation

WEBGRO server (<https://simlab.uams.edu>) [19] was used to run MD simulations of the top three complexes. The topology files of the ligands were obtained using PRODRG server [20] (<http://davapc1.bioch.dundee.ac.uk/cgi-bin/prodrgr>). Each top complex was directly solvated in simple point charge (SPC) waters, followed by GROMOS96 43a1 force field, and then Na⁺ and Cl⁻ ions were utilized to achieve a neutral system. To optimize energy minimization, the steepest descent algorithm was used. To sustain a constant temperature and volume, we used NVT dynamics. The simulation was performed in 1000 steps for 100 ns, with the temperature of the Noose-hover set to 300 K.

3. Result and Discussion

Previous studies have shown the success of fluoroquinolones and the existence of other exploitable ligand-binding pockets in gyrase suggesting the importance of new gyrase-specific inhibitors. In a study by Rahimi *et al.* [6], they have used the simocyclinone D8 (SD8), which inhibits both gyrase DNA binding and supercoiling reaction, hence it acts as a competitive inhibitor for DNA binding sites. Using this mechanism of inhibition, structural similarity search and molecular docking studies were carried out to identify new molecules for DNA gyrase inhibition using SD8 structure.

Setzer *et al.* [7] have screened 561 known antibacterial phytochemicals listed in the Dictionary of Natural Products with the help of docking studies with six bacterial protein targets (peptide deformylase, DNA gyrase/topoisomerase IV, UDP-galactose mutase, protein tyrosine phosphatase, cytochrome P450 CYP121, and NAD⁺-dependent DNA ligase) of *E. coli*. *E. coli* peptide deformylase (EcPDF), *E. coli* topoisomerase IV (EcTopoIV), and *E. coli* DNA ligase (EcLigA) were found to be most susceptible protein targets, based upon docking energies, for phytochemical ligands. The researchers have also tried working on the structural modifications in templates obtained from natural sources that contribute to better activity like cyclothialidines and haloemodin analogues to treat bacterial infections [8]. Various research papers reveal that we can discover a novel scaffold of DNA gyrase inhibitors by combining multiple machine learning methods and target-based approaches [9].

3.1. Pharmacokinetics, Bioavailability and Drug-Likeliness Property Assessment of the Selected Phytochemicals

The antagonistic activity of the ligands with a protein does not assure that a ligand is acceptable as a potential drug candidate; hence evaluating the pharmacokinetic properties such as ADME

(absorption, distribution, metabolism, and excretion) is considered one of the most effective screening techniques in drug development, since it helps ascertain the safety and efficacy of the ligands. The lack of information regarding pharmacokinetics and toxicity profiles can be the major reasons for the rejection of lead molecules in clinical trials. Lipinski's theoretical statements are considered a thumb-rule for evaluating its pharmacokinetics, drug-likeness, and assessing if a ligand with specific pharmacological and biological characteristics in the living organism can be converted into an orally administered drug [21]. Pharmacokinetic properties were evaluated and used for the initial screening of 302 bioactive compounds. Compounds with zero violation were considered best lead molecules, while others were eliminated from further analysis, culminating in 240 molecules. Lipophilicity, size, polarity, solubility, flexibility, and saturation were used to evaluate these compounds for their potential as oral drugs. An extensive study was carried out using the SwissADME tool, which provides a graphical illustration in the form of radar, which is based on various physicochemical properties. 165 molecules showed significant deviation from these parameters, implying that these ligands are unlikely to be considered orally bioavailable, while 75 molecules were identified as orally bioavailable.

3.2. Molecular Docking of the Selected Protein Ligand Complex

The emergence of virtual screening methodologies has provided great momentum to the research focusing on drug discovery. It has become a powerful tool in pharmaceutical research since it aims to determine the conformation of ligands within the binding site with a considerable degree of precision [22]. In the current analysis, we studied interactions between Topoisomerase II and lead molecules using the AutoDock Vina tool, which helped screen 75 bioactive molecules along with the standard anti-tubercular drugs. The interaction between the receptor and ligand was demonstrated in the form of binding affinity. The graphical representation of the six best screened compounds along with standard drugs is depicted in pictorial form in Figure 2.

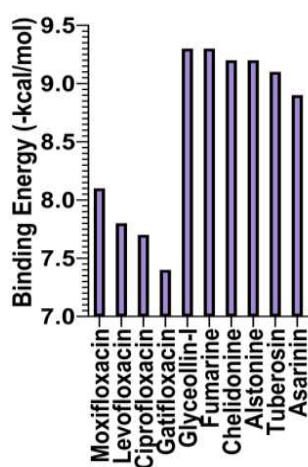


Figure 2. Graphical representation of the binding energy of the top six phytochemicals and standard drugs.

Table 1. Molecular docking data represented in terms of binding energy (ΔG) in kcal/mole for Topoisomerase II receptor with the phytochemicals and standard drugs. (Center Alignment of data in table).

Sr. No	Ligand	Binding Energy (ΔG) (kcal/mol)
1	Glyceollin-I	-9.3
2	Fumarine	-9.3
3	Chelidonine	-9.2
4	Alstonine	-9.2
5	Tuberosin	-9.1
6	Asarinin	-8.9
7	Moxifloxacin	-8.1
8	Levofloxacin	-7.8
9	Ciprofloxacin	-7.7
10	Gatifloxacin	-7.4

The binding energies of the 75 bioactive compounds ranged from -2.9 to -9.3 kcal/mol, whereas the four standard drug binding energies ranged from -7.4 to -8.1 kcal/mol. A threshold was set at -8.5 kcal/mol to determine the potential inhibitors, and only six molecules (Table 1), namely Glyceollin-I, Fumarine, Chelidonine, Alstonine, Tuberosin, and Asarinin, qualified that requirement. Thus, the selected phytochemicals performed better than the standard drugs. Moreover, amongst the four standard drugs, Moxifloxacin, which is currently recommended for the treatment of multidrug-resistant tuberculosis, showed the least binding energy of -8.1 kcal/mol. It interacted with the receptor by forming conventional H-bond, alkyl, and pi-alkyl bonds in Figure 3(A) shows 3D representation of the position of Moxifloxacin within the cavity of Topoisomerase II receptor, followed by the 3D interaction diagram of Moxifloxacin with Topoisomerase II receptor, (B) 2D interaction diagram of Moxifloxacin docked in the binding pockets of Topoisomerase II receptor visualized using Discovery Studio 2020, (C) 3D structure of Moxifloxacin. The binding energies of Levofloxacin and Ciprofloxacin were -7.8 and -7.7 kcal/mol, respectively. They also formed conventional H-bond, carbon H-bond, pi-alkyl, and alkyl bonds with the receptor. Figure 4 shows (A) 3D representation of the position of Levofloxacin within the cavity of Topoisomerase II receptor, followed by the 3D interaction diagram of Levofloxacin with Topoisomerase II receptor, (B) 2D interaction diagram of Levofloxacin docked in the binding pockets of Topoisomerase II receptor visualized using Discovery Studio 2020, (C) 3D structure of Levofloxacin and figure 5 shows (A) 3D representation of the position of Ciprofloxacin within the cavity of Topoisomerase II receptor, followed by the 3D interaction diagram of Ciprofloxacin with Topoisomerase II receptor, (B) 2D interaction diagram of Ciprofloxacin docked in the binding pockets of Topoisomerase II receptor visualized using Discovery Studio 2020, (C) 3D structure of Ciprofloxacin. In addition to this, an unfavorable donor-donor bond was observed between Ciprofloxacin and the receptor, indicating repulsive forces and inferring that the complex is unstable. Lastly, Gatifloxacin revealed binding energy of -7.4 kcal/mol, which is lowest than the rest of the standard drugs. There were three types of non-covalent interactions, and one covalent interaction was observed: conventional H-bond, carbon H-

bond and pi-alkyl interactions between the drug and receptor as shown in Figure 6(A) 3D representation of the position of Gatifloxacin within the cavity of Topoisomerase II receptor, followed by the 3D interaction diagram of Gatifloxacin with Topoisomerase II receptor, (B) 2D interaction diagram of Gatifloxacin docked in the binding pockets of Topoisomerase II receptor visualized using Discovery Studio 2020, (C) 3D structure of Gatifloxacin.

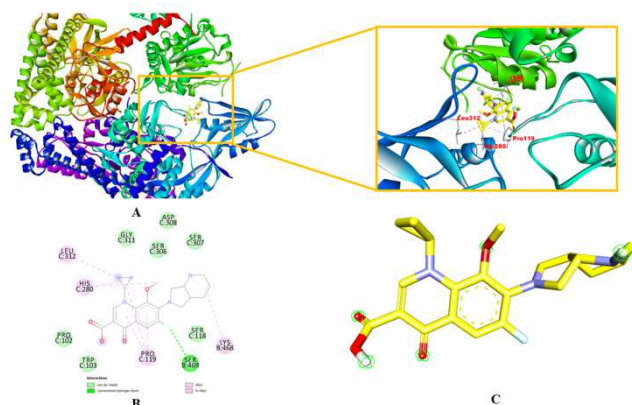


Figure 3. Docking Poses of Topoisomerase II with Moxifloxacin.

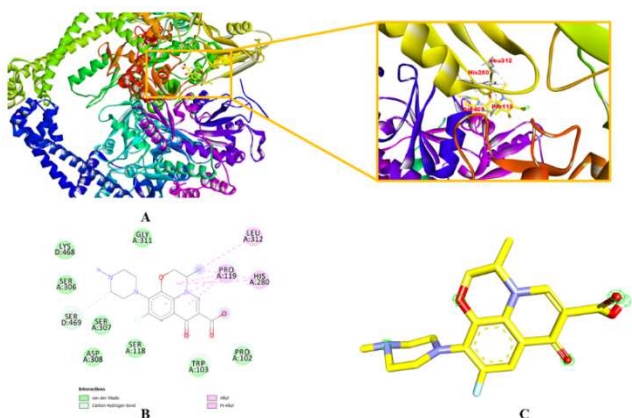


Figure 4. Docking Poses of Topoisomerase II with Levofloxacin.

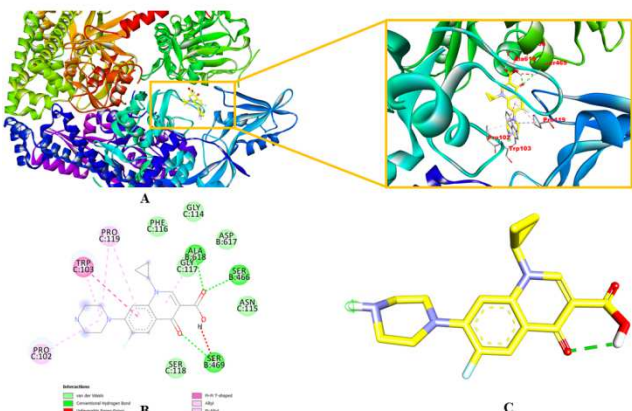


Figure 5. Docking Poses of Topoisomerase II with Ciprofloxacin.

Glyceollin-I is one of the most essential phytoalexins found in soybeans. It has been observed that Glyceollin-I acts

as an antimicrobial drug candidate against *Pseudomonas syringae* through in silico approach. In the present study, Glyceollin-I exhibited the least binding energy of all the molecules, -9.3 kcal/mol. LYS 468 of the B chain formed a conventional H-bond, whereas the C chain residue SER 306 formed a carbon H-bond with the ligand. ASP 304 of the C chain and ARG 471 of the B chain interacted with the ligand by forming pi-cation and pi anion bonds. A pi-alkyl bond was observed between LYS 430 of the B chain residue and the ligand. The C chain residues: SER 118, PRO 119, ASP 122, SER 307, and the B chain residues: ARG 429, ASP 444, ARG 446, SER 469, and SER 473 were found to interact with the ligand via Van der Waals forces shown in Figure 7 (A) 3D representation of the position of Glyceollin-I within the cavity of Topoisomerase II receptor, followed by the 3D interaction diagram of Glyceollin-I with Topoisomerase II receptor, and (B) 2D interaction diagram of Glyceollin-I docked in the binding pockets of Topoisomerase II receptor visualized using Discovery Studio 2020, (C) 3D structure of Glyceollin-I.

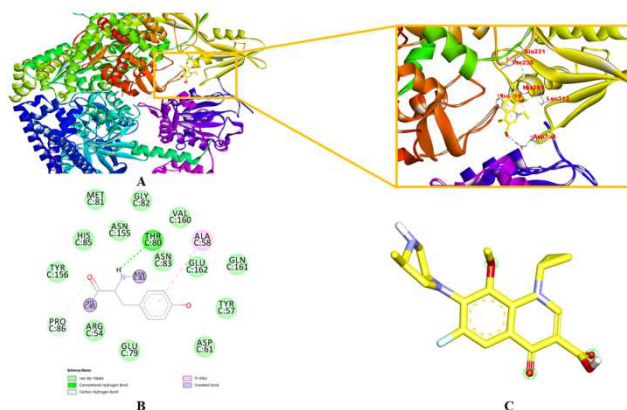


Figure 6. Docking Poses of Topoisomerase II with Gatifloxacin.

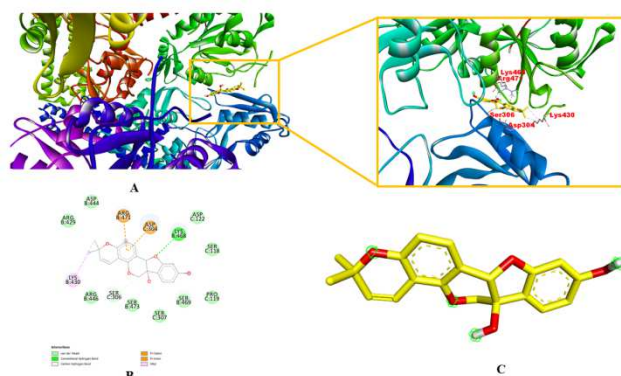


Figure 7. Docking Poses of Topoisomerase II with Glyceollin-I.

Fumarine, also known as Protopine, belongs to the family of organic compounds known as protopine alkaloids [23]. UkrainTM, an anticancer drug formulated from the extract of the plant *Chelidonium majus* L. [24], contains Fumarine as one of its active compounds [25]. It has been reported to possess antimicrobial activity against *Bacillus cereus*, *Staphylococcus aureus*, *Bacillus subtilis*, *Escherichia coli*,

Pseudomonas aeruginosa, and *Erwinia carotovora* [26]. The binding energy of Fumarine was -9.3 kcal/mol, similar to that of Glyceollin-I. It formed two conventional H-bonds with ASP 308 of the C chain. The C chain residue HIS 280 and the B chain residue ALA 618 interacted with the ligand by forming alkyl and pi-alkyl bonds. The C chain residues GLY 114, ASN 115, GLY 117, SER 118, PRO 119, SER 306, SER 307, GLY 311, LEU 312, and the B chain residues SER 466, SER 469, and ASP 617 were found to interact with the ligand through Van der Waals forces as shown in Figure 8(A) 3D representation of the position of Fumarine within the cavity of Topoisomerase II receptor, followed by the 3D interaction diagram of Fumarine with Topoisomerase II receptor, and (B) 2D interaction diagram of Fumarine docked in the binding pockets of Topoisomerase II receptor visualized using Discovery Studio 2020, (C) 3D structure of Fumarine.

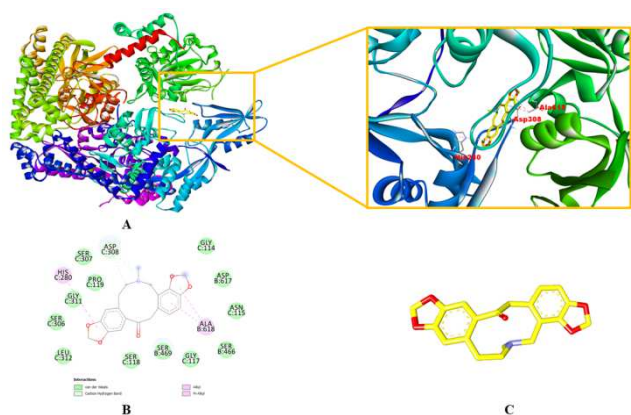


Figure 8. Docking Poses of Topoisomerase II with Fumarine.

the ligand. PRO 102 of the A chain and ALA 618 of the D chain formed alkyl and pi-alkyl bonds with the ligand. ALA 100, TRP 103, ASP 111, GLY 114, ASN 115, PHE 116, SER 118 of the A chain, and SER 469 of the D chain were observed to interact through Van der Waals forces with the ligand. In Figure 9(A) 3D representation of the position of Chelidonine within the cavity of Topoisomerase II receptor, followed by the 3D interaction diagram of Chelidonine with Topoisomerase II receptor, (B) 2D interaction diagram of Chelidonine docked in the binding pockets of Topoisomerase II receptor visualized using Discovery Studio 2020, (C) 3D structure of Chelidonine. Alstonine is an indole alkaloid [31]. It exhibited *in vivo* antimalarial activity in a preliminary study performed by Gandhi and Vinayak et al, [32]. Moreover, animal model studies have proven it as anxiolytic and antipsychotic properties [33]. It displayed -9.2 kcal/mol as its binding energy in our study. SER 466 and ALA 618 of the B chain residue formed conventional H-bonds with the ligand. TRP 103 of the C chain was seen to interact with the ligand via a Pi-Pi T shaped bond. Pi-alkyl and alkyl bonds were observed between PRO 102, PRO 119 residues, with the ligand. ASN 115 of the C chain interacted with the ligand via carbon H-bond. The remaining amino acid residues of the B and C chain: SER 469, ASP 617, PHE 116, GLY 117, SER 118, ASP 122, HIS 280, SER 306, GLY 311, and LEU 312 were found to interact through Van der Waals forces with the ligand as shown in Figure 10(A) 3D representation of the position of Alstonine within the cavity of Topoisomerase II receptor, followed by the 3D interaction diagram of Alstonine with Topoisomerase II receptor, (B) 2D interaction diagram of Alstonine docked in the binding pockets of Topoisomerase II receptor visualized using Discovery Studio 2020, (C) 3D structure of Alstonine.

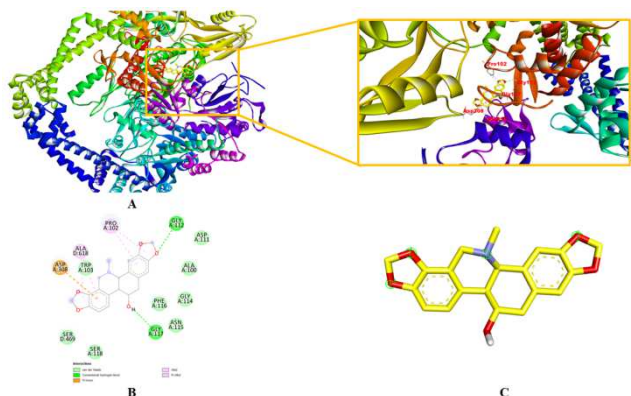


Figure 9. Docking Poses of Topoisomerase II with Chelidonine.

Chelidonine, an isoquinoline alkaloid, considered as the principal alkaloid part of *Chelidonium majus*. Chelidonine, like Fumarine, is one of the active ingredients in UkrainTM [25]. It has known to possess anti-tumour [27], anti-inflammatory [28], anti-oxidant [29], and anti-microbial [30] properties. In our study, it revealed -9.2 kcal/mol binding energy. GLY 112 and GLY 117 of the A chain residues were seen to interact with the ligand through conventional H-bonds. A pi-anion bond was observed between ASP 308 and

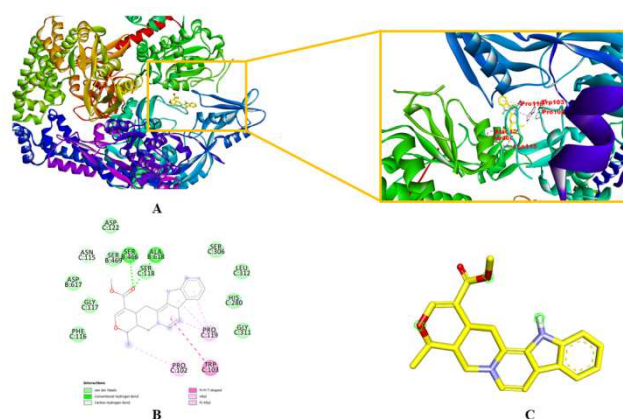


Figure 10. Docking Poses of Topoisomerase II with Alstonine.

Tuberosin belongs to the class of compounds referred to as pterocarpan [34]. It is one of *Pueraria tuberosa*'s active ingredients, and it has been shown to have antioxidant properties [35]. In this present study, it showed the binding energy of -9.1 kcal/mol. It formed three conventional H-bonds with SER 118, ASP 122 of the A chain, and LYS 468 of the D chain. It even formed alkyl bonds with PRO 119 of the A chain. The following A chain residues: GLY 120, HIS

280, ASP 304, SER 306, SER 307, ASP 308, GLY 311, LEU 312, and the D chain residues: SER 469, ARG 471, and SER 473 were observed to interact through Van der Waals forces with the ligand as shown in Figure 11(A) 3D representation of the position of Tuberostin within the cavity of Topoisomerase II receptor, followed by the 3D interaction diagram of Tuberostin with Topoisomerase II receptor, (B) 2D interaction diagram of Tuberostin docked in the binding pockets of Topoisomerase II receptor visualized using Discovery Studio 2020, (C) 3D structure of Tuberostin.

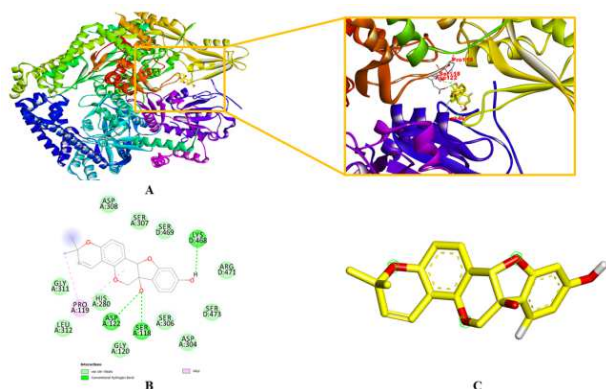


Figure 11. Docking Poses of Topoisomerase II with Tuberostin.

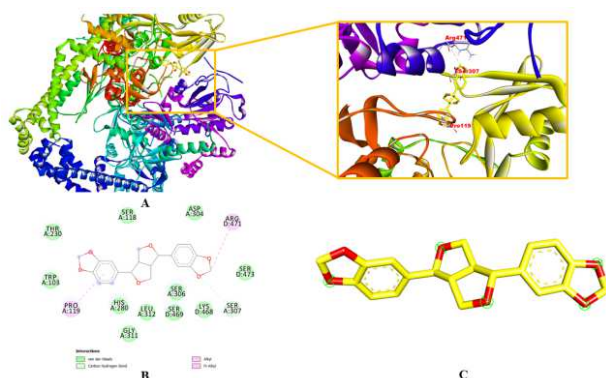


Figure 12. Docking Poses of Topoisomerase II with Asarinin.

Asarinin, a furofuran lignan, found in *Asarum* species [36]. It has been known that Asarinin is known to be potent against nontuberculous *Mycobacterium* strains (*M. smegmatis*, *M. abscessus*, *M. chelonae*, *M. marinum*, *M. avium* A5) in an *in vitro* study, with MIC values ranging from 35 to 140 µg/mL [37]. In this study, Asarinin manifested binding energy of -9.1 kcal/mol. A carbon H-bond was observed between the ligand and the SER 307 residue of the A chain. It also formed a pi-alkyl and alkyl bond with PRO 119 of the A chain, and ARG 471 of the D chain. TRP 103, SER 118, THR 230, HIS 280, ASP 304, SER 306, GLY 311, and LEU 312 of the A chain residues and LYS 468, SER 469, and SER 473 of the D chain residues interacted with the ligand through Van der Waals forces as shown in Figure 12(A) 3D representation of the position of Asarinin within the cavity of Topoisomerase II receptor, followed by the 3D interaction diagram of Asarinin with Topoisomerase II receptor, (B) 2D interaction diagram of Asarinin docked in the binding pockets of Topoisomerase II receptor visualized using Discovery Studio 2020, (C) 3D structure of Asarinin.

3.3. Toxicity Prediction of the Shortlisted Phytochemicals

Toxicity is thought to be responsible for approximately 1/3rd of drug candidate attrition and is a major contributor to the high cost of drug production, particularly when found late in clinical trials or after marketing [38]. New compound toxicity testing is important for the drug discovery process. In silico approaches have many advantages, including the potential to analyse hypothetical compounds, their low cost, and the fact that such simulated tests are usually focused on human data, eliminating the issue of interspecies transferability [39]. ProTox-II is one of the computational tools that use a total of 33 models for the estimation of different toxicity endpoints such as acute toxicity, hepatotoxicity, carcinogenicity, mutagenicity, and so on. The toxicity profiles of both the control drugs and the shortlisted phytochemicals are shown in Table 2.

Table 2. Toxicity results of Shortlisted phytochemicals and standard drugs. (Center Alignment of data in table).

Drugs	Toxicity Class	LD50 value (mg/kg)	Hepatotoxicity	Carcinogenicity	Mutagenicity
Glyceollin-I	4	500	Inactive	Inactive	Inactive
Fumarine	4	940	Inactive	Active	Active
Chelidonine	4	460	Inactive	Active	Active
Alstonine	3	215	Inactive	Inactive	Inactive
Tuberostin	4	500	Inactive	Inactive	Inactive
Asarinin	3	1500	Inactive	Active	Inactive
Moxifloxacin	4	2000	Inactive	Inactive	Active
Levofloxacin	4	1478	Inactive	Inactive	Active
Ciprofloxacin	4	2000	Inactive	Inactive	Active
Gatifloxacin	4	2000	Inactive	Inactive	Inactive

From Table 2, it can be observed that all the control drugs belong to the class four toxicity. In the case of the LD50 value, Moxifloxacin, Ciprofloxacin, and Gatifloxacin each had an LD50 of 2000mg/kg, while Levofloxacin had an LD50 of 1478mg/kg. In comparison, the toxicity profiles of the phytochemicals revealed that Glyceollin-I, Fumarine,

Chelidonine and Tuberostin belong to the class four toxicity while Alstonine and Asarinin belong to class three toxicity indicating that they might be toxic. LD50 values of these phytochemicals ranged from 460mg/kg for Chelidonine to 500mg/kg for Glyceollin-I and Tuberostin, and 940mg/kg for Fumarine. Asarinin has the highest LD50 value of

1500mg/kg, despite being classified as a type three toxicity. Hepatotoxicity was inactive for all the candidate drugs as well as the control drugs. Carcinogenicity was inactive in all the control drugs. In contrast, active carcinogenicity was found in the case of Fumarine, Asarinin, and Chelidonine. Mutagenicity was active in all the control drugs except Gatifloxacin. Likewise, Fumarine and Chelidonine were shown to be mutagenic as compared to other compounds. Despite the fact that fluoroquinolones have been predicted to be safe by the ProTox server, they have been associated with numerous adverse reactions, including minor neurotoxic reactions, musculoskeletal reactions, CNS, GI tract reactions, cardiovascular reactions, and many others [40, 41]. Therefore, the flavonoids Glyceollin-I and Tuberosin, and alkaloid Alstonine were safe and were evaluated further using MD simulation.

3.4. Molecular Dynamic Simulation of Best Protein Ligand Complex

MD simulation is one of the most valuable analyses in structure-based drug design as they provide a comprehensive understanding of the receptor-ligand complex's stability. The RMSD plots of the receptor and

three complexes, receptor-Glyceollin-I, receptor-Tuberosin, and receptor- Alstonine complex, were evaluated in this analysis to investigate their stability profiles during simulations. The RMSD value of the receptor-Glyceollin-I complex was between 0.1 and 3.1 nm, with one sharp peak of up to 7nm at 35ns and another of 8.5 nm 55ns. Furthermore, the RMSD plot of Glyceollin-I complex revealed multiple fluctuations and failed to achieve stability during 100 ns simulation time. The RMSD value of the receptor-Tuberosin complex was in the 0.01–13.5nm range. In comparison with the RMSD plot of glyceollin-I complex, this system achieved stability after 70ns, however, the RMSD value is considerably high (up to 15nm). Therefore, this indicates that the receptor-Glyceollin-I and Tuberosin complex is unstable, making it inadequate for further *in vitro* and *in vivo* analysis. On the contrary, as shown in Figure 13, the RMSD value of the receptor- Alstonine complex was in the range of 0.2 – 0.8 nm. Even though the RMSD plot of the Alstonine complex displayed variations, it was able to achieve equilibration at 80ns. This indicates that the receptor-Alstonine complex was stable and hence can be considered for the development of a drug against the Topoisomerase II receptor of *M. tb*.

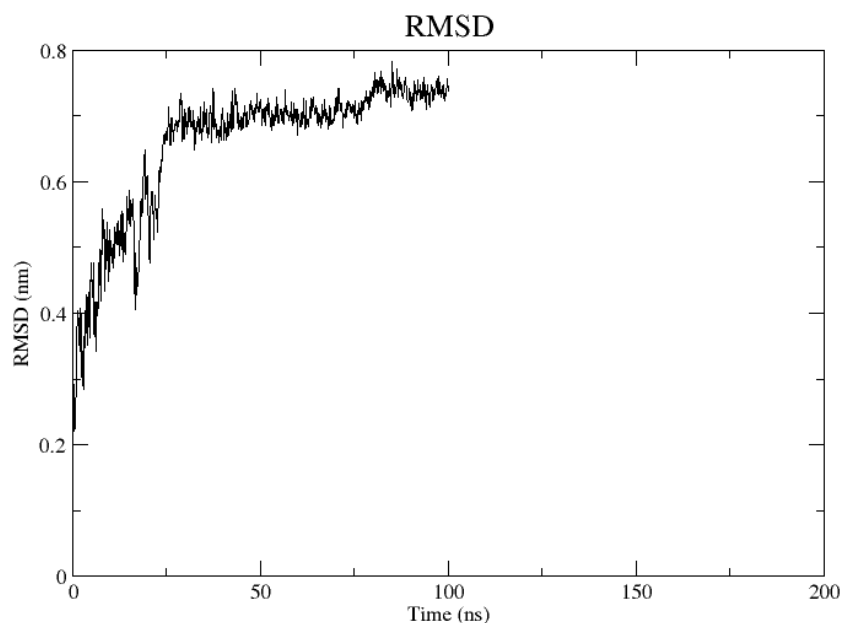


Figure 13. RMSD plot of the Topoisomerase II receptor-Alstonine complex.

4. Conclusion

This study, which employs a bioinformatic method, lays the groundwork for discovering, testing, and developing a new tuberculosis treatment. Theoretical evaluations of binding affinities (kcal/mol) of several phytochemical ligands were conducted in order to evaluate their potency and find a potential lead molecule for developing a potential medication.

In the present research, a virtual screening approach was used to ascertain a potential inhibitor against the

topoisomerase II complex of *Mtb*. As a filtering tool, the Lipinski rule of five was used, which resulted in 240 bioactive molecules. Using the Bioavailability Radar tool, these 240 molecules were further screened. Seventy-five molecules were found to be orally bioavailable, which were then further docked with the protein. Docking analysis revealed six molecules, namely Glyceollin-I, Fumarine, Chelidonine, Alstonine, Tuberosin, and Asarinin, as potential inhibitors against the receptor. Interestingly, these compounds outperformed the standard drugs, suggesting that they can be a viable alternative to these well-established

standard drugs. Furthermore, the MD analysis of the safe ligands revealed Alstonine to be the most stable molecule. Thus, our research finding enhances the significance of this compound as an attractive drug candidate for the treatment of multidrug-resistant tuberculosis. Therefore, the selected molecule can be further validated with *in vitro* and *in vivo* studies. The study's findings suggest the relevance of these compounds as potential leads for treating *Mycobacterium tuberculosis*, which could help medicinal chemists and pharmaceutical professionals discover and synthesize more potent therapeutic options in the future. It also stimulates the study's *in vitro* and *in vivo* evaluation for proposed developed drugs in order to validate the computational results.

References

- [1] S. Kumar *et al.*, "The phytochemical bergenin as an adjunct immunotherapy for tuberculosis in mice," *J. Biol. Chem.*, vol. 294, no. 21, pp. 8555–8563, 2019, doi: 10.1074/jbc.RA119.008005.
- [2] K. A. Abrahams *et al.*, "Anti-tubercular derivatives of rhein require activation by the monoglyceride lipase Rv0183," *Cell Surf.*, vol. 6, no. April, 2020, doi: 10.1016/j.tcs.2020.100040.
- [3] M. Mori *et al.*, "An Overview on the Potential Antimycobacterial Agents Targeting Serine/Threonine Protein Kinases from *Mycobacterium tuberculosis*," *Curr. Top. Med. Chem.*, vol. 19, no. 9, pp. 646–661, 2019, doi: 10.2174/1568026619666190227182701.
- [4] H. Tomioka, "Current status and perspective on drug targets in tubercle bacilli and drug design of antituberculous agents based on structure-activity relationship," *Current pharmaceutical design*, vol. 20, no. 27, United Arab Emirates, pp. 4305–4306, 2014, doi: 10.2174/1381612819666131118203915.
- [5] M. A. Reiche, D. F. Warner, and V. Mizrahi, "Targeting DNA replication and repair for the development of novel therapeutics against tuberculosis," *Front. Mol. Biosci.*, vol. 4, no. NOV, pp. 1–18, 2017, doi: 10.3389/fmolb.2017.00075.
- [6] H. Rahimi, A. Najafi, H. Eslami, B. Negahdari, and M. M. Moghaddam, "Identification of novel bacterial DNA gyrase inhibitors: An in silico study," *Research in Pharmaceutical Sciences*, vol. 11, no. 3, pp. 233–242, 2016.
- [7] M. S. Setzer, J. Sharifi-Rad, and W. N. Setzer, "The search for herbal antibiotics: An in-silico investigation of antibacterial phytochemicals," *Antibiotics*, vol. 5, no. 3, 2016, doi: 10.3390/antibiotics5030030.
- [8] T. Khan, K. Sankhe, V. Suvana, A. Sherje, K. Patel, and B. Dravyakar, "DNA gyrase inhibitors: Progress and synthesis of potent compounds as antibacterial agents," *Biomed. Pharmacother.*, vol. 103, no. March, pp. 923–938, 2018, doi: 10.1016/j.biopha.2018.04.021.
- [9] L. Li, X. Le, L. Wang, Q. Gu, H. Zhou, and J. Xu, "Discovering new DNA gyrase inhibitors using machine learning approaches," *RSC Adv.*, vol. 5, no. 128, pp. 105600–105608, 2015, doi: 10.1039/c5ra22568j.
- [10] V. Nagaraja, A. A. Godbole, S. R. Henderson, and A. Maxwell, "DNA topoisomerase I and DNA gyrase as targets for TB therapy," *Drug Discov. Today*, vol. 22, no. 3, pp. 510–518, 2017, doi: 10.1016/j.drudis.2016.11.006.
- [11] J. K. Kumar, A. G. Devi Prasad, and V. Chaturvedi, "Phytochemical screening of five medicinal legumes and their evaluation for *in vitro* anti-tubercular activity," *Ayu*, vol. 35, no. 1, pp. 98–102, Jan. 2014, doi: 10.4103/0974-8520.141952.
- [12] H. M. Berman, K. Henrick, H. Nakamura (2003) Announcing the worldwide Protein Data Bank *Nature Structural Biology* 10 (12): 980.
- [13] "Dr. Duke's Phytochemical and Ethnobotanical Databases." <https://phytochem.nal.usda.gov/phytochem/search>.
- [14] Schrödinger LLC, "The PyMOL Molecular Graphics System, Version 2.4," *Schrödinger LLC*. 2020.
- [15] A. Daina, O. Michielin, and V. Zoete, "SwissADME: A free web tool to evaluate pharmacokinetics, drug-likeness and medicinal chemistry friendliness of small molecules," *Sci. Rep.*, vol. 7, no. January, pp. 1–13, 2017, doi: 10.1038/srep42717.
- [16] G. M. Morris *et al.*, "AutoDock4 and AutoDockTools4: Automated docking with selective receptor flexibility," *J. Comput. Chem.*, vol. 30, no. 16, pp. 2785–2791, Dec. 2009, doi: 10.1002/jcc.21256.
- [17] O. Trott and A. J. Olson, "AutoDock Vina: improving the speed and accuracy of docking with a new scoring function, efficient optimization, and multithreading," *J. Comput. Chem.*, vol. 31, no. 2, pp. 455–461, Jan. 2010, doi: 10.1002/jcc.21334.
- [18] M. N. Drwal, P. Banerjee, M. Dunkel, M. R. Wettig, and R. Preissner, "ProTox: A web server for the in silico prediction of rodent oral toxicity," *Nucleic Acids Res.*, vol. 42, no. W1, pp. 3–8, 2014, doi: 10.1093/nar/gku401.
- [19] Abraham, Mark James, Teemu Murtola, Roland Schulz, Szilárd Páll, Jeremy C Smith, Berk Hess, and Erik Lindahl. 2015. "GROMACS: High Performance Molecular Simulations through Multi-Level Parallelism from Laptops to Supercomputers." *SoftwareX* 1–2: 19–25. <https://doi.org/https://doi.org/10.1016/j.softx.2015.06.001>.
- [20] Schüttelkopf, Alexander W, and Daan M F van Aalten. 2004. "PRODRG: A Tool for High-Throughput Crystallography of Protein-Ligand Complexes." *Acta Crystallographica. Section D, Biological Crystallography* 60 (Pt 8): 1355–63. <https://doi.org/10.1107/S0907444904011679>.
- [21] C. A. Lipinski, "Lead- and drug-like compounds: The rule-of-five revolution," *Drug Discov. Today Technol.*, vol. 1, no. 4, pp. 337–341, 2004, doi: 10.1016/j.ddtec.2004.11.007.
- [22] L. G. Ferreira, R. N. Dos Santos, G. Oliva, and A. D. Andricopulo, *Molecular docking and structure-based drug design strategies*, vol. 20, no. 7. 2015.
- [23] S. A. SAEED, A. H. GILANI, R. U. MAJOO, and B. H. SHAH, "ANTI-THROMBOTIC AND ANTI-INFLAMMATORY ACTIVITIES OF PROTOPINE," *Pharmacol. Res.*, vol. 36, no. 1, pp. 1–7, 1997, doi: <https://doi.org/10.1006/phrs.1997.0195>.
- [24] E. Ernst and K. Schmidt, "Ukrain - a new cancer cure? A systematic review of randomised clinical trials," *BMC Cancer*, vol. 5, p. 69, Jul. 2005, doi: 10.1186/1471-2407-5-69.

- [25] Q. Lei, H. Liu, Y. Peng, and P. Xiao, "In silico target fishing and pharmacological profiling for the isoquinoline alkaloids of *Macleaya cordata* (Bo Luo Hui)," *Chinese Med. (United Kingdom)*, vol. 10, no. 1, pp. 1–20, 2015, doi: 10.1186/s13020-015-0067-4.
- [26] Y. Su, S. Li, N. Li, L. Chen, J. Zhang, and J. Wang, "Seven alkaloids and their antibacterial activity from *Hypecoum erectum* L.," *J. Med. Plant Res.*, vol. 5, no. 22, pp. 5428–5432, 2011.
- [27] R. Herrmann, J. Roller, C. Polednik, and M. Schmidt, "Effect of chelidonine on growth, invasion, angiogenesis and gene expression in head and neck cancer cell lines," *Oncol. Lett.*, vol. 16, no. 3, pp. 3108–3116, 2018, doi: 10.3892/ol.2018.9031.
- [28] J. Lenfeld, M. Kroutil, E. Marsalek, J. Slavík, V. Preininger, and V. Simánek, "Antiinflammatory activity of quaternary benzophenanthridine alkaloids from *Chelidonium majus*," *Planta Med.*, vol. 43, no. 2, pp. 161–165, 1981, doi: 10.1055/s-2007-971493.
- [29] J. E. Park *et al.*, "Alkaloids from *Chelidonium majus* and their inhibitory effects on LPS-induced NO production in RAW264.7 cells," *Bioorganic Med. Chem. Lett.*, vol. 21, no. 23, pp. 6960–6963, 2011, doi: 10.1016/j.bmcl.2011.09.128.
- [30] S. Zielińska *et al.*, "The Activity of Isoquinoline Alkaloids and Extracts from *Chelidonium majus* against Pathogenic Bacteria and *Candida* sp.," *Toxins (Basel)*, vol. 11, no. 7, Jul. 2019, doi: 10.3390/toxins11070406.
- [31] E. Elisabetsky and L. Costa-Campos, "The alkaloid alstonine: A review of its pharmacological properties," *Evidence-based Complement. Altern. Med.*, vol. 3, no. 1, pp. 39–48, 2006, doi: 10.1093/ecam/nek011.
- [32] M. Gandhi and V. K. Vinayak, "Preliminary evaluation of extracts of *Alstonia scholaris* bark for in vivo antimalarial activity in mice," *J. Ethnopharmacol.*, vol. 29, no. 1, pp. 51–57, Apr. 1990, doi: 10.1016/0378-8741(90)90097-d.
- [33] L. Costa-Campos, D. R. Lara, D. S. Nunes, and E. Elisabetsky, "Antipsychotic-like profile of alstonine," *Pharmacol. Biochem. Behav.*, vol. 60, no. 1, pp. 133–141, 1998, doi: 10.1016/S0091-3057(97)00594-7.
- [34] B. S. Joshi and V. N. Kamat, "Tuberosin, a new pterocarpan from *Pueraria tuberosa* DC.," *J. Chem. Soc. Perkin 1*, vol. 9, pp. 907–911, 1973, doi: 10.1039/p19730000907.
- [35] N. Pandey and Y. B. Tripathi, "Antioxidant activity of tuberosin isolated from *Pueraria tuberosa* Linn.," *J. Inflamm.*, vol. 7, pp. 1–8, 2010, doi: 10.1186/1476-9255-7-47.
- [36] Y. Ma, K. Xu, S. Wang, and Y. Han, "Simultaneous Determination of Two Epimeric Furofuran Lignans (Sesamin and Asarinin) of *Asarum heterotropoides* Extract in Rat Plasma by LC/MS/MS: Application to Pharmacokinetic Study," *J. Chromatogr. Sci.*, vol. 52, no. 8, pp. 793–798, 2013, doi: 10.1093/chromsci/bmt114.
- [37] R. O. Bussey *et al.*, "Antimycobacterial furofuran lignans from the roots of *anemopsis californica*," *Planta Med.*, vol. 80, no. 6, pp. 498–501, 2014, doi: 10.1055/s-0034-1368352.
- [38] F. Peter Guengerich, "Mechanisms of drug toxicity and relevance to pharmaceutical development," *Drug Metab. Pharmacokinet.*, vol. 26, no. 1, pp. 3–14, 2011, doi: 10.2133/dmpk.DMPK-10-RV-062.
- [39] A. Vedani and M. Smiesko, "In silico toxicology in drug discovery - Concepts based on three-dimensional models," *ATLA Altern. to Lab. Anim.*, vol. 37, no. 5, pp. 477–496, 2009, doi: 10.1177/026119290903700506.
- [40] B. A. Lipsky and C. A. Baker, "Fluoroquinolone toxicity profiles: A review focusing on newer agents," *Clin. Infect. Dis.*, vol. 28, no. 2, pp. 352–364, 1999, doi: 10.1086/515104.
- [41] R. Stahlmann and H. Lode, "Toxicity of quinolones," *Drugs*, vol. 58, no. SUPPL. 2, pp. 37–42, 1999, doi: 10.2165/00003495-199958991-00005.